NASA-CR-853

E2

NASA CONTRACTOR REPORT

NASA CR-853

NASA CR-853

DISTRIBUTION STATEMENT A
Approved for Public Release
Distribution Unlimited

Reproduced From
Best Available Copy

THE MAXIMUM RESPONSE OF RECTANGULAR PLATES TO RANDOM EXCITATION

by Richard L. Barnoski

Prepared by
MEASUREMENT ANALYSIS CORPORATION
Los Angeles, Calif.
for George C. Marshall Space Flight Center

20011022 113

NATIONAL AERONAUTICS AND SPACE ADMINISTRATION • WASHINGTON, D. C. • SEPTEMBER 1967

NASA CR-853

THE MAXIMUM RESPONSE OF RECTANGULAR PLATES TO RANDOM EXCITATION

By Richard L. Barnoski

Distribution of this report is provided in the interest of information exchange. Responsibility for the contents resides in the author or organization that prepared it.

Prepared under Contract No. NAS 8-20020 by
MEASUREMENT ANALYSIS CORPORATION
Los Angeles, Calif.

for George C. Marshall Space Flight Center

NATIONAL AERONAUTICS AND SPACE ADMINISTRATION

For sale by the Clearinghouse for Federal Scientific and Technical Information
Springfield, Virginia 22151 – CFSTI price $3.00

ABSTRACT

This report considers empirical solutions to the first-passage or single-highest-peak (SHP) problem for a distributed elastic structure with rectangular geometry subjected to both stationary and a specific form of nonstationary random excitation. The structure is a flat, homogeneous, uniform, square plate and the applied stationary excitation is white noise perfectly correlated in both space and time. The nonstationary excitation is a rectangular noise burst with a unity correlation in both space and time. The structure and the excitation are simulated electrically and peak response data are collected for (1) simply supported boundary conditions at all edges and (2) rigidly clamped boundary conditions at all edges. These response data are used to establish probability curves yielding an estimate of the probability that the maximum response, for a finite time interval, remains below a preselected threshold level.

CONTENTS

1. INTRODUCTION

The SHP (single-highest-peak) problem generally refers to predicting the maximum response a mechanical system may achieve, within a finite time interval, when subjected to stationary, broad-band white noise excitation. It is noted that the maximum response need not necessarily correspond to a peak amplitude in the response time history. The solution rests with determining $P_M(|\beta| \leq \beta_o, T)$ which is the probability that the absolute value of the response β remains below a threshold level β_o within the time interval T. The term β is a dimensionless ratio of the maximum amplitude to RMS response of the system and T is the time interval over which the response is observed. The β response may be a positive maximum value β^+, a negative maximum value β^-, or an absolute maximum value $|\beta|$ and the RMS response is the system RMS response to stationary white noise excitation perfectly correlated in space and time. For this discussion, only solutions involving $|\beta|$ values are shown.

For a single degree-of-freedom system, the SHP problem has been examined in detail by various investigators using both simulation and analytical procedures as is discussed in References listed at the end of this report. Solutions acceptable for practical applications have been cleverly determined not only for stationary white noise excitation (References 1 and 7), but also for white noise applied as a step function (Reference 5) and for particular noise bursts as well (References 4 and 8). It is judicious to examine some of the established results for the vibration of a single degree-of-freedom system before discussing the SHP problem for a distributed elastic structure.

2. RESULTS FOR A SINGLE DEGREE-OF-FREEDOM SYSTEM

A linear single degree-of-freedom mechanical system (also called a linear mechanical oscillator) is shown as Figure 1

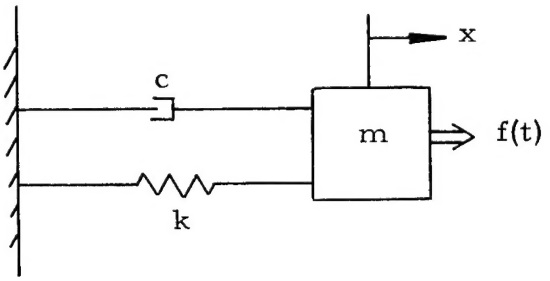

Figure 1. A Single Degree-of-Freedom Mechanical System

The dynamic behavior of this system is defined by the equation of motion

$$m\ddot{x} + c\dot{x} + kx = f(t) \tag{1}$$

where m corresponds to the mass, c the viscous damping coefficient, k the spring constant and f(t) a forcing function applied to the mass. In an alternate form, this equation may be written as

$$\ddot{x} + 2\zeta\omega_n\dot{x} + \omega_n^2 x = \frac{f(t)}{m} \tag{2}$$

where

$$\frac{c}{m} = 2\zeta\omega_n$$

$$\frac{k}{m} = \omega_n^2 = (2\pi f_n)^2 \tag{3}$$

and ζ is the damping factor and ω_n the undamped natural frequency of the system. For f(t) equal to a simple harmonic forcing function, say $f(t) = f_o \sin \omega t$, the forced displacement response x(t) is

$$x(t) = \frac{H(\omega)}{m\omega_n^2} f_o \sin \omega t \tag{4}$$

where the magnification factor $H(\omega)$ is defined in complex form by

$$H(\omega) = \frac{1}{1 - \left(\frac{\omega}{\omega_n}\right)^2 + i\, 2\zeta \frac{\omega}{\omega_n}} \tag{5}$$

For f(t) equal to an arbitrary deterministic function of time, the response may be calculated in the following ways

$$x(t) = \frac{1}{2\pi} \int_{-\infty}^{\infty} \frac{1}{m\omega_n^2} H(\omega)\, F(\omega)\, e^{i\omega t}\, d\omega = \int_0^t h(\tau)\, f(t - \tau)\, d\tau \tag{6}$$

where $F(\omega)$ is the Fourier Transform of $f(t)$ and $h(\tau)$ is the system response to a unit impulse excitation. The solution obtained by integrating over ω is a Fourier integral solution while the form given by integrating over τ is a convolution integral solution. The Fourier integral gives the solution $x(t)$ as a superposition of steady-state responses and the convolution integral gives the solution as a superposition of free vibration responses.

The output response of a lightly damped single degree-of-freedom system wherein $f(t)$ is stationary broadband white noise excitation is shown as Figure 2. The undamped natural frequency of the mechanical system is assumed large compared with the half-power bandwidth AND the bandwidth of the input spectrum is assumed wide in comparison to the system half-power bandwidth and includes f_n. It is further implied the system has achieved stationarity in its response and we are observing the response beginning at an arbitrary instant of time.

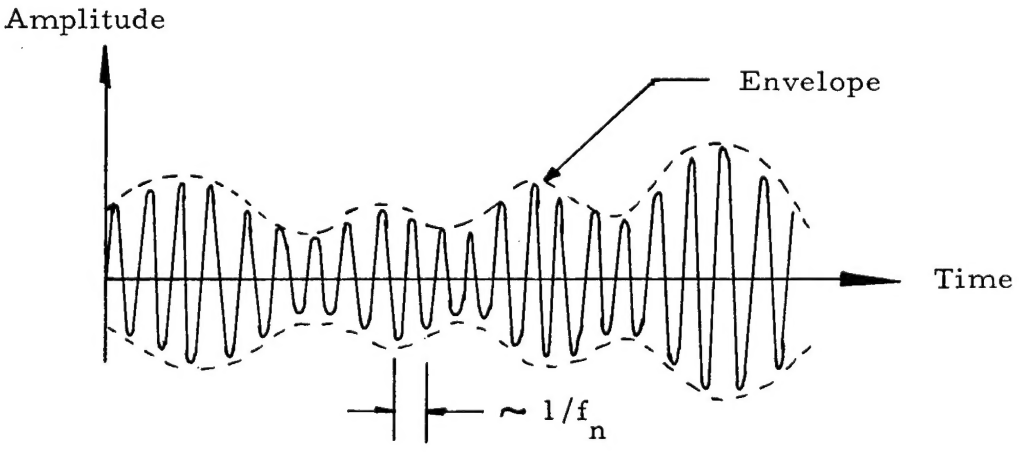

Figure 2. Response of a Lightly Damped Mechanical Oscillator to Broadband Stationary Random Excitation

This response appears as a sinusoid (at the frequency f_n) with a slowly varying random amplitude and random phase. The average number of zero crossings per second $E[N_o]$ is approximately

$$E[N_o] = \frac{1}{\pi}\sqrt{\frac{\omega_1^2 + \omega_1\omega_2 + \omega_2^2}{3}} \approx \frac{\omega_n}{\pi} \tag{7}$$

where ω_1 and ω_2 are interpreted as the half-power point frequencies in radians per second. The mean square displacement response ψ_x^2 is

$$\psi_x^2 = \frac{\pi G_o Q}{2 m^2 \omega_n^3} I_n \tag{8}$$

where

$$Q = \frac{1}{2\zeta}$$

and G_o is the magnitude of the input spectrum with units of $lb^2/rad/sec$. The term I_n (see page 80 of Reference 6 and Reference 11) is a dimensionless coefficient ranging from zero to one with its exact value being dependent upon (1) the damping factor ζ and (2) the ratio of the cutoff frequency ω_c of the input spectrum to ω_n as shown in Figure 3. Similarly, the mean square velocity response $\psi_{\dot{x}}^2$ is

$$\psi_{\dot{x}}^2 = \frac{\pi G_o Q}{2 m^2 \omega_n} II_n \tag{9}$$

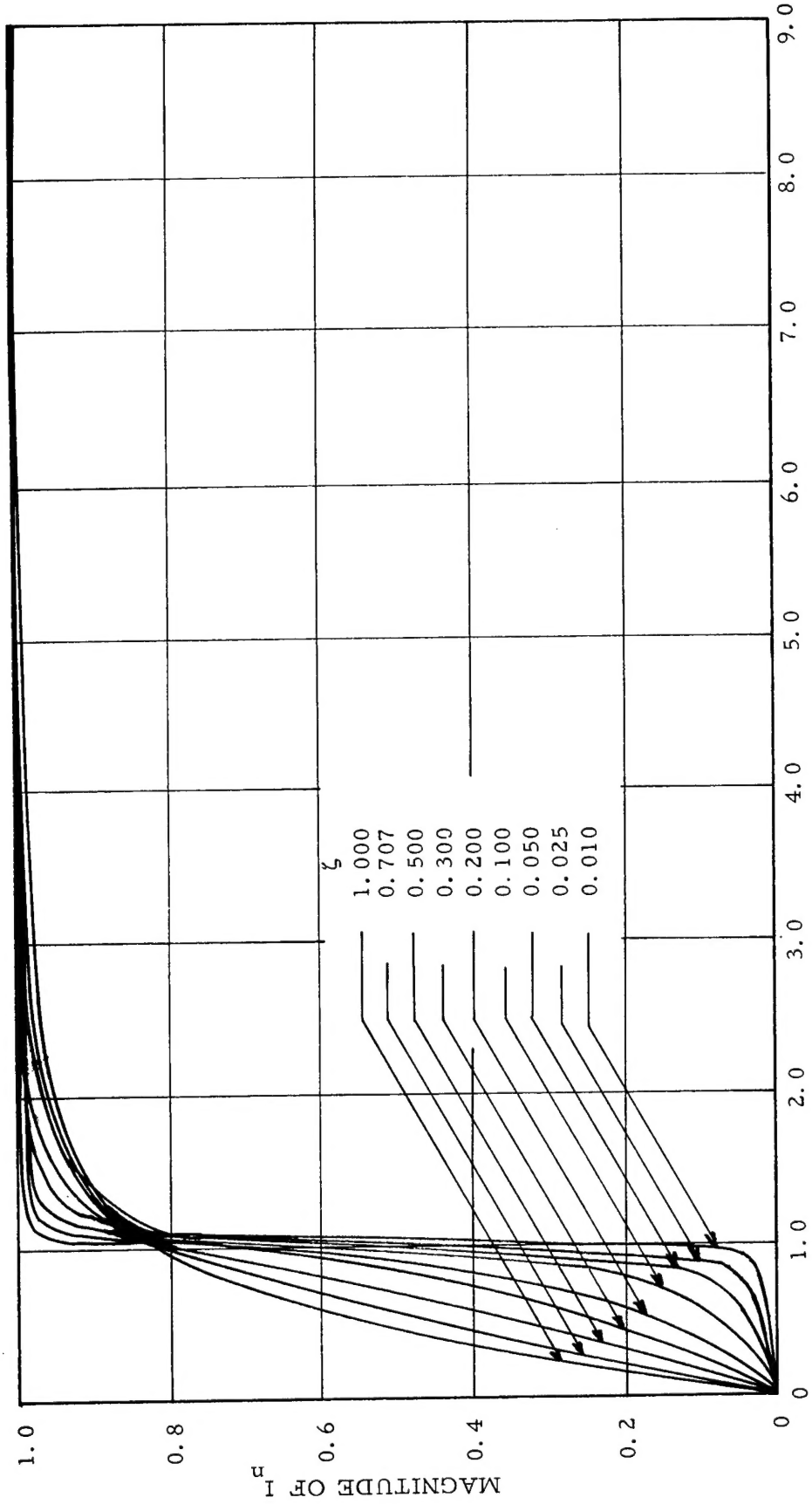

Figure 3. Numerical Value of I_n

where the dimensionless coefficient II_n is shown as Figure 4. For high Q systems ($\zeta < 0.010$), both I_n and II_n are nearly zero for ω_c/ω_n somewhat less than one; they rapidly approach unity as ω_c/ω_n becomes slightly greater than one and converge to unity as $\omega_c/\omega_n \rightarrow \infty$. This behavior implies the mechanical system acts as a highly selective band-pass filter for both displacement and velocity and admits frequency components principally near ω_n. By selecting I_n and II_n as unity, upper limits* for ψ_x^2 and $\psi_{\dot{x}}^2$ are calculated.

The autocorrelation function for the displacement response is

$$R_x(\tau) \simeq \frac{\pi Q G_o}{2 m^2 \omega_n^3} e^{-\zeta \omega_n \tau} \left(\cos \omega_d t + \frac{\zeta}{\sqrt{1 - \zeta^2}} \sin \omega_d t \right) \qquad (10)$$

where ω_d is the damped natural frequency of the system and related to ω_n as $\omega_d = \omega_n \sqrt{1 - \zeta^2}$. The magnitude of this function at $\tau = 0$ yields the mean square displacement response

$$R_x(0) = \psi_x^2 = \frac{\pi Q G_o}{2 m^2 \omega_n^3}$$

which is identical to Eq. (8) with I_n equal to unity.

---

*The mean square acceleration response may be developed in a similar manner and, in general, tends to be divergent as $\omega_c/\omega_n > 1$ and becomes unbounded as $\omega_c/\omega_n \rightarrow \infty$.

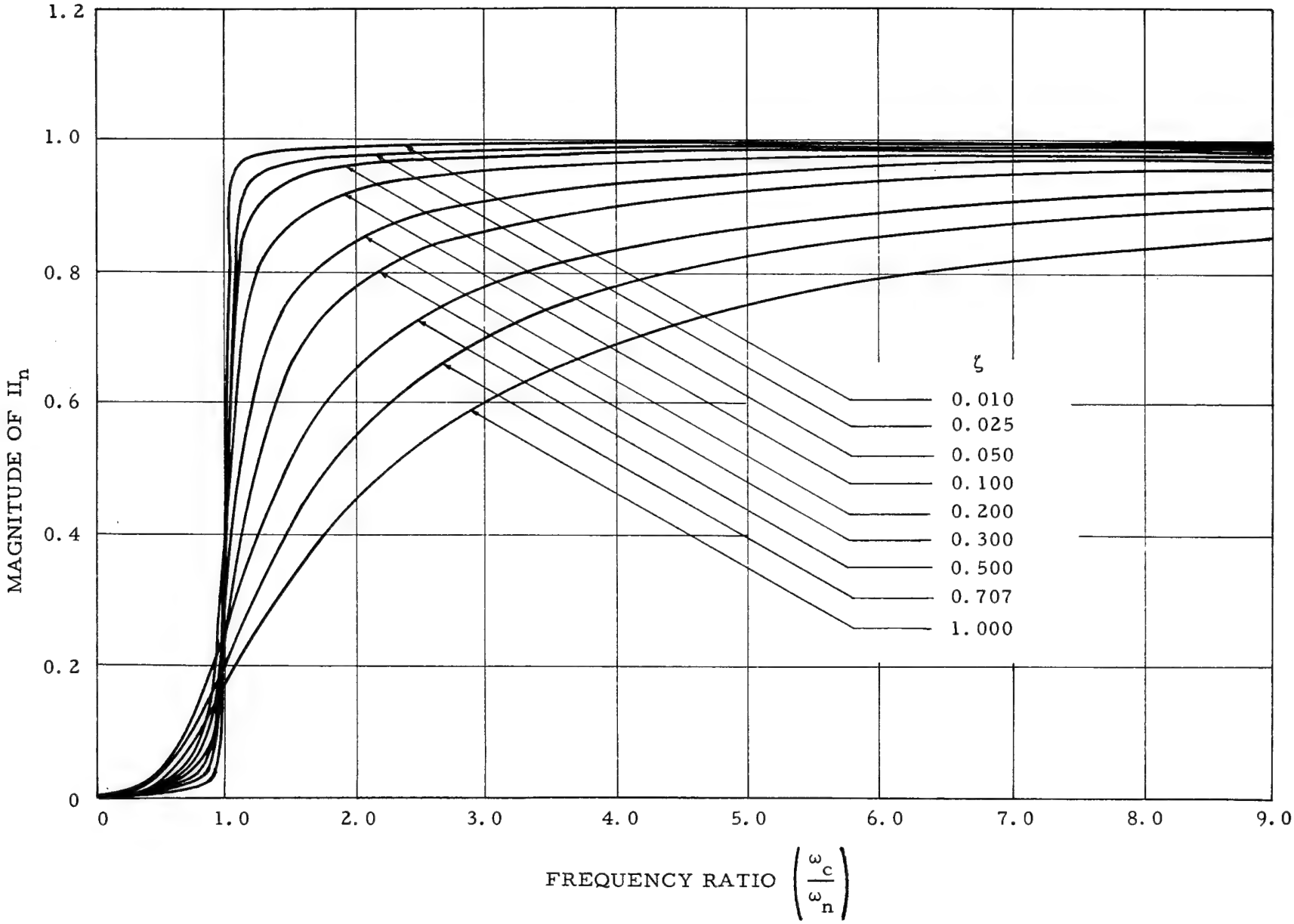

Figure 4. Numerical Value of II_n

The time lapse $\Delta\tau$ for the amplitude of $R_x(\tau)$ to decay to $\frac{1}{e}$ times its initial amplitude is given by

$$\Delta\tau = \frac{Q}{\pi f_n} = \frac{1}{\zeta\omega_n} \tag{11}$$

and is called the correlation time or correlation interval (Reference 5). This time interval corresponds to the time lapse for the free vibration of a lightly damped single degree-of-freedom system to decay to $\frac{1}{e}$ times an initial amplitude x_o.

For a white noise excitation, the probability density function of the response at any instant of time is Gaussian (Normal). The probability density of the envelope of the peaks is Rayleigh. The probability density of the individual peak amplitudes is, likewise, nearly Rayleigh and becomes precisely Rayleigh when the damping becomes sufficiently small to define an infinitely narrow bandpass at f_n.

The probability density of the response maxima during a finite observation time is neither Gaussian nor Rayleigh and forms the crux of the SHP problem. A solution for this probability distribution function is given in Reference 10 as

$$\hat{P}_M(|\beta| \leq \beta_o, T) \simeq A_o e^{-\alpha_o Q \omega_n T} \qquad T > \tau_{cor} \tag{12}$$

where A_o is a constant whose magnitude is dependent upon the initial conditions of the system, and τ_{cor} denotes the time lapse for the autocorrelation function to decay to a negligible value. For most applications with $\beta_0 \geq 2$, A_o may be assumed equal to unity with trivial error. The

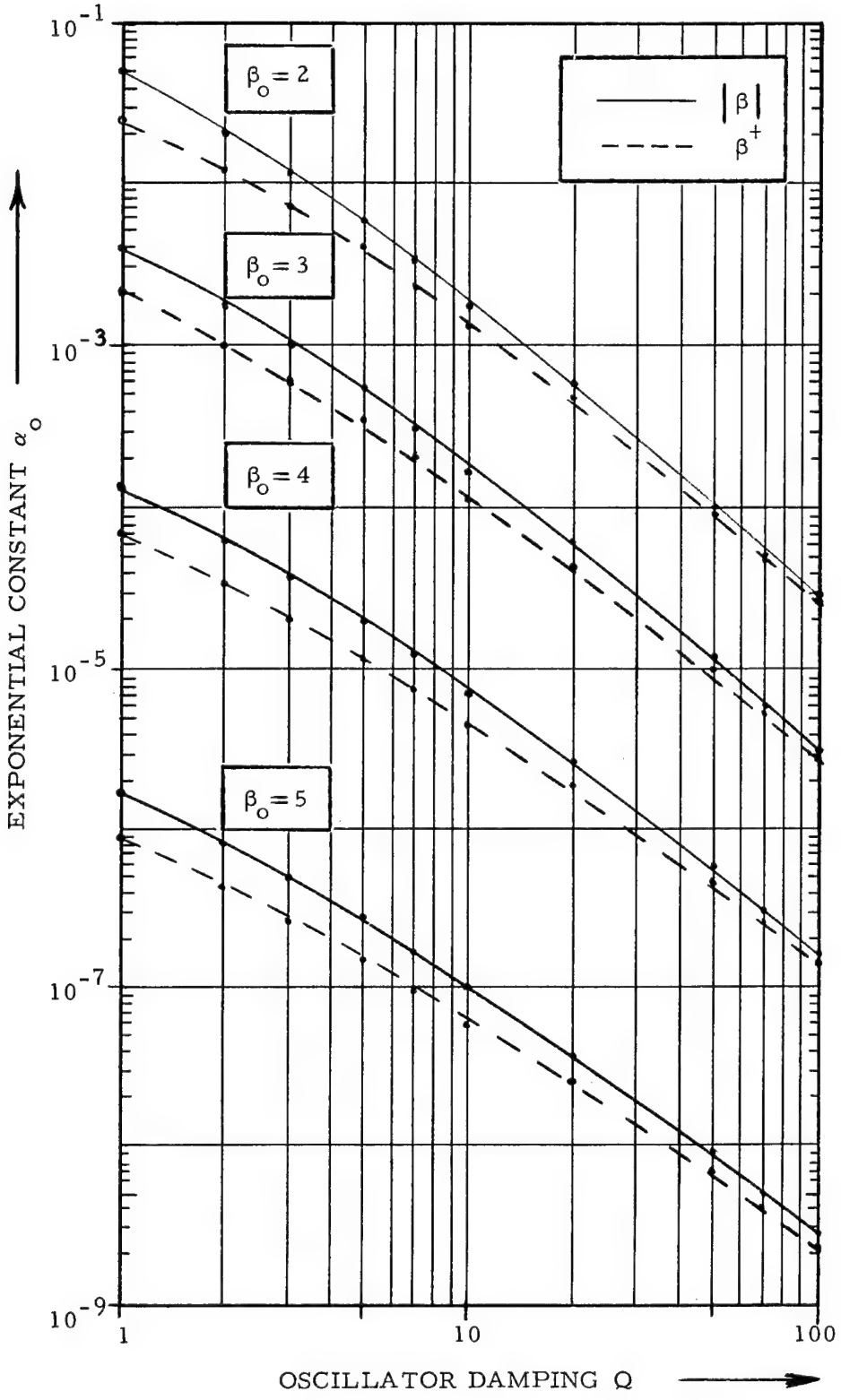

Figure 5. Plot of Exponential Constant α_o

term α_o is dependent upon the system damping Q and a preselected level of the β_o ratio. Plots of α_o versus Q are shown in Figure 5 as families of curves in β_o for both β^+ and $|\beta|$. This figure in conjunction with Eq. (12) provides a theoretical solution to the SHP problem for a linear mechanical oscillator.

Empirical solutions to this problem have been determined using techniques amenable to digital and analog computation. By means of an active electrical analog simulation (differential amplifier circuits), the results* shown as Figures 6, 7, 8 and 9 have been obtained. Figures 6 and 7 are families of plots in Q of the dimensionless time parameter $f_n T/Q$ versus $|\beta|$ for $\hat{P}_M(|\beta| \leq \beta_o) = 0.50$ and 0.95. These data may be compared directly with the results of Figure 5 by restating Eq. (12) in the form

$$\alpha_o = - \frac{\ln [P_M(|\beta| \leq \beta_o)]}{2\pi Q^2 \left[\frac{f_n T}{Q}\right]} \tag{13}$$

and evaluating this expression in the following manner

*These data are partially from Reference 4 and partially from independent analog studies carried out after the writing of Reference 4. Additional data were obtained from a digital simulation study sponsored by Mr. E. H. Schell of AFFDL, Wright-Patterson Air Force Base, Ohio. These digital results tend to substantiate the shown analog data although the β results for the higher probability values were consistently lower (within 10% and generally not more than 5%).

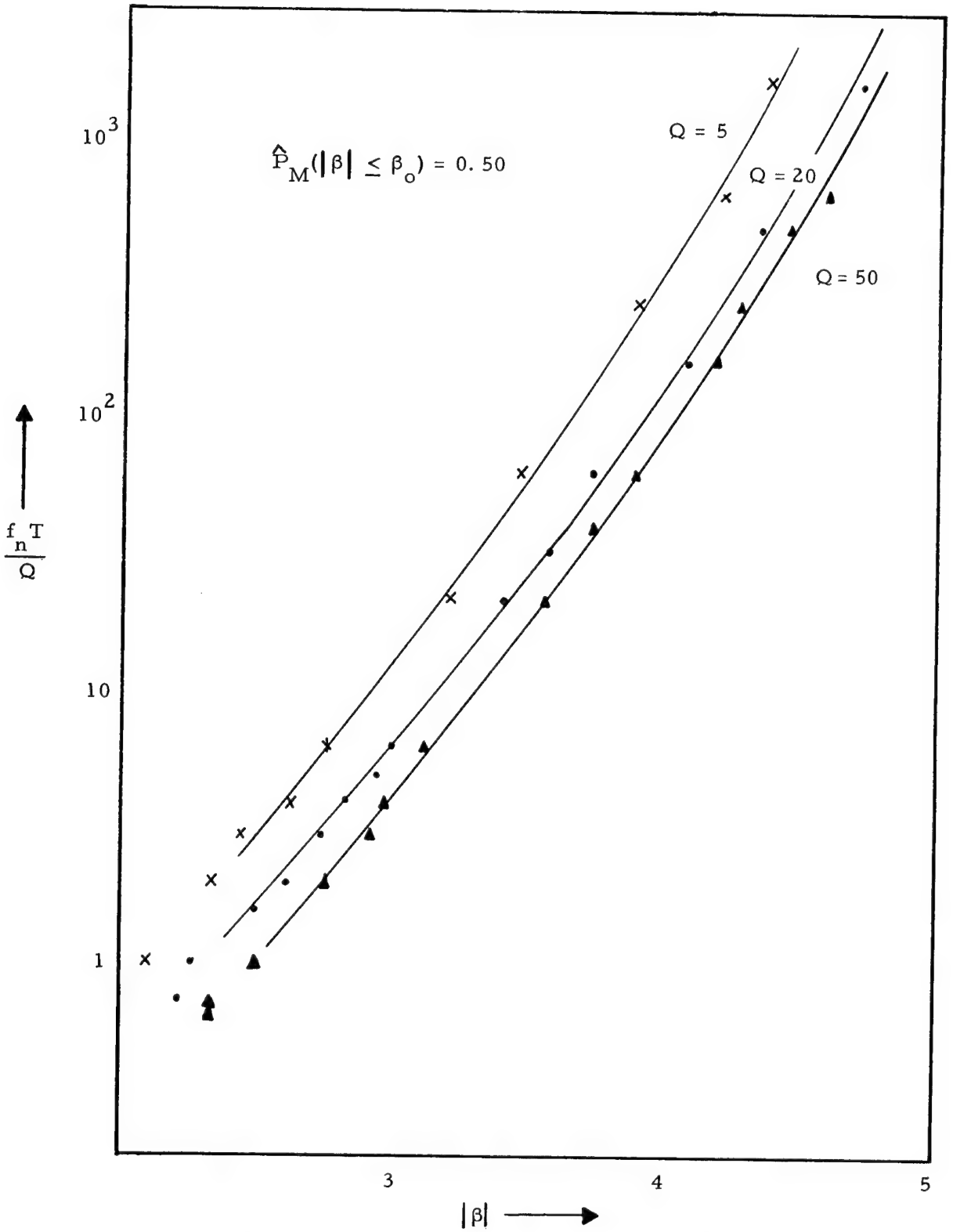

Figure 6. Response Maxima of a Single Degree-of-Freedom System to Stationary White Noise

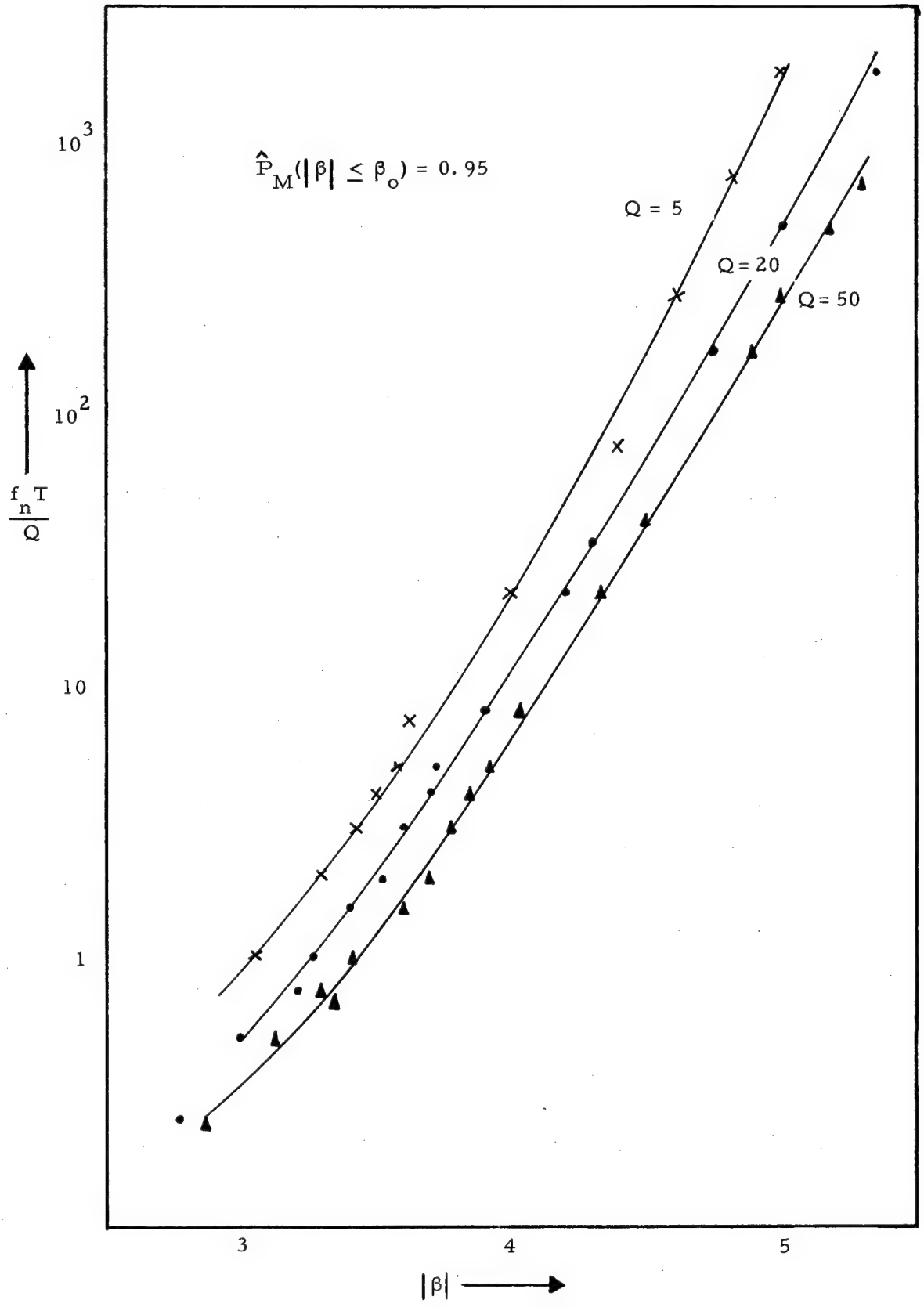

Figure 7. Response Maxima of a Single Degree-of-Freedom System to Stationary White Noise

$$\alpha_o = - \frac{\ln [0.50]}{2\pi Q^2 \left[\frac{f_n T}{Q}\right]}$$

$$\alpha_o = - \frac{\ln [0.95]}{2\pi Q^2 \left[\frac{f_n T}{Q}\right]}$$

The data values for $\beta_o = 3$ and $\beta_o = 4$ in Figure 6 and for $\beta_o = 3$, $\beta_o = 4$ and $\beta_o = 5$ in Figure 7 agree closely with their equivalent values in Figure 5. It may thus be concluded that these analog results definitively support the theoretical solution of Eq. (12).

Figure 8 is a set of plots in Q of $|\beta|$ versus $f_n T/Q$ for $\hat{P}_M(|\beta| \leq \beta_o) = 0.95$ and $\hat{P}_M(|\beta| \leq \beta_o) = 0.50$. Only curves for $Q = 20$ and $Q = 50$ are shown since these values are considered to be more typical of damping in physical structures, and thus, of most interest. These curves are exploded views of Figures 6 and 7 for $f_n T/Q \leq 5$ and find application wherein the time interval T may be relatively short. The larger $|\beta|$ values are associated with the lower damping ratios for all $f_n T/Q$ with the sharpest rate of increase noted for $f_n T/Q$ ranging from 0 to 3. It is observed that β_o values of 3 for $\hat{P}_M(|\beta| \leq \beta_o) = 0.50$ and β_o values of 4 for $\hat{P}_M(|\beta| \leq \beta_o) = 0.95$ are to be expected where $f_n T/Q \geq 5$.

Figure 9 shows $|\beta|$ versus $f_n T/Q$ plots of the average maxima of $|\beta|$ for $Q = 20$ and $Q = 50$. These curves are very nearly the same as those for $\hat{P}_M(|\beta| \leq \beta_o) = 0.50$ in Figure 8 with one exception. The data for $Q = 20$ appears to become numerically equivalent with that for $Q = 50$

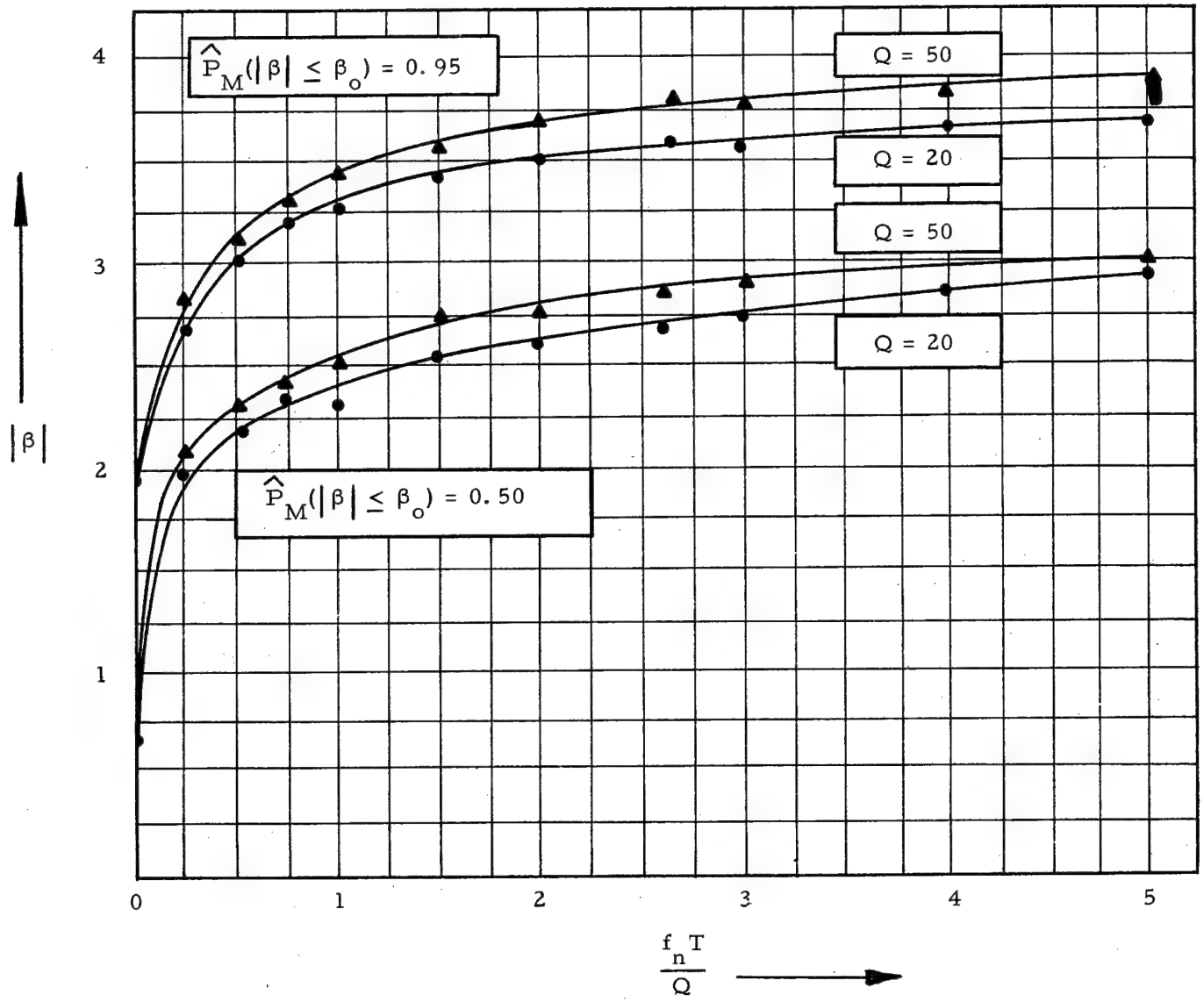

Figure 8. Maximum Response of a Single Degree-of-Freedom System to Stationary White Noise

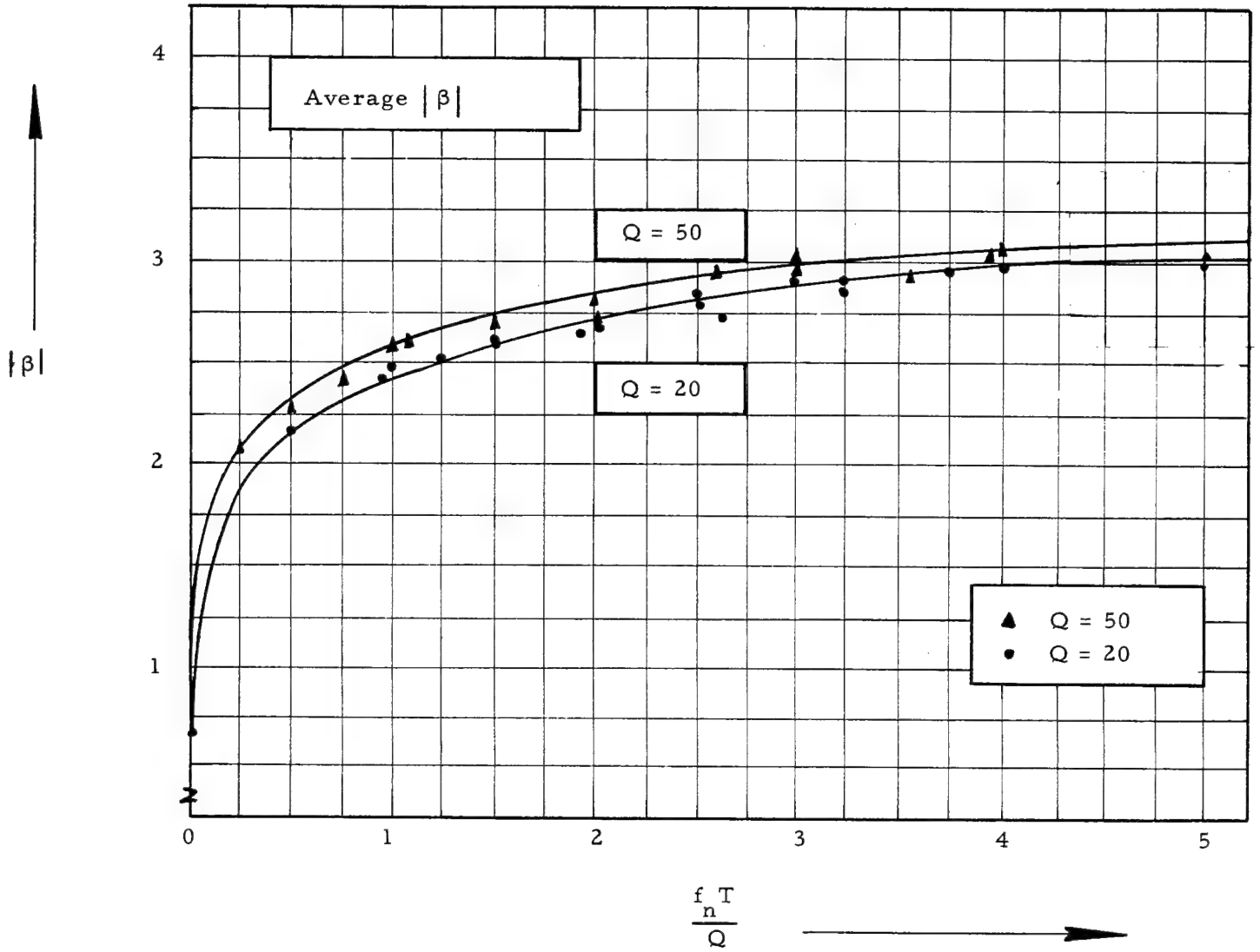

Figure 9. Average Response Maxima of Single Degree-of-Freedom System to Stationary White Noise

where $f_n T/Q \geq 4$. From these data, the median and average values of $|\beta|$ for $Q = 50$ tend to become very nearly the same. It is suggested that a practical estimate of the average maximum response may be determined by using the $|\beta|$ versus $f_n T/Q$ plot for $Q = 50$.

The maximum response of a simple oscillator to shaped noise bursts also has been examined by an active analog simulation as discussed in References 4 and 8. The noise burst excitation may be written as

$$f(t) = E(t)\, n(t) \tag{14}$$

where $E(t)$ is a specifically defined envelope function and $n(t)$ is the output response of a random noise generator with a white noise spectrum of magnitude G_o. Data from these studies are shown as Figures 10 and 11 where $|\beta|$ is the dimensionless ratio of the maximum response to the RMS response and $f_n \tau/Q$ is the dimensionless time ratio where τ is a time duration of the input burst of noise. The RMS response is the output response of the oscillator to broadband white noise wherein $E(t) = 1$. By normalizing the β response in this way, time varying RMS considerations are avoided. These data suggest the noise burst response maxima become relatively the same as that for the stationary response when $f_n \tau/Q \simeq 1.5$. Thus, plots such as these may be used to establish criteria for the conditions under which an oscillator achieves stationarity in its response.

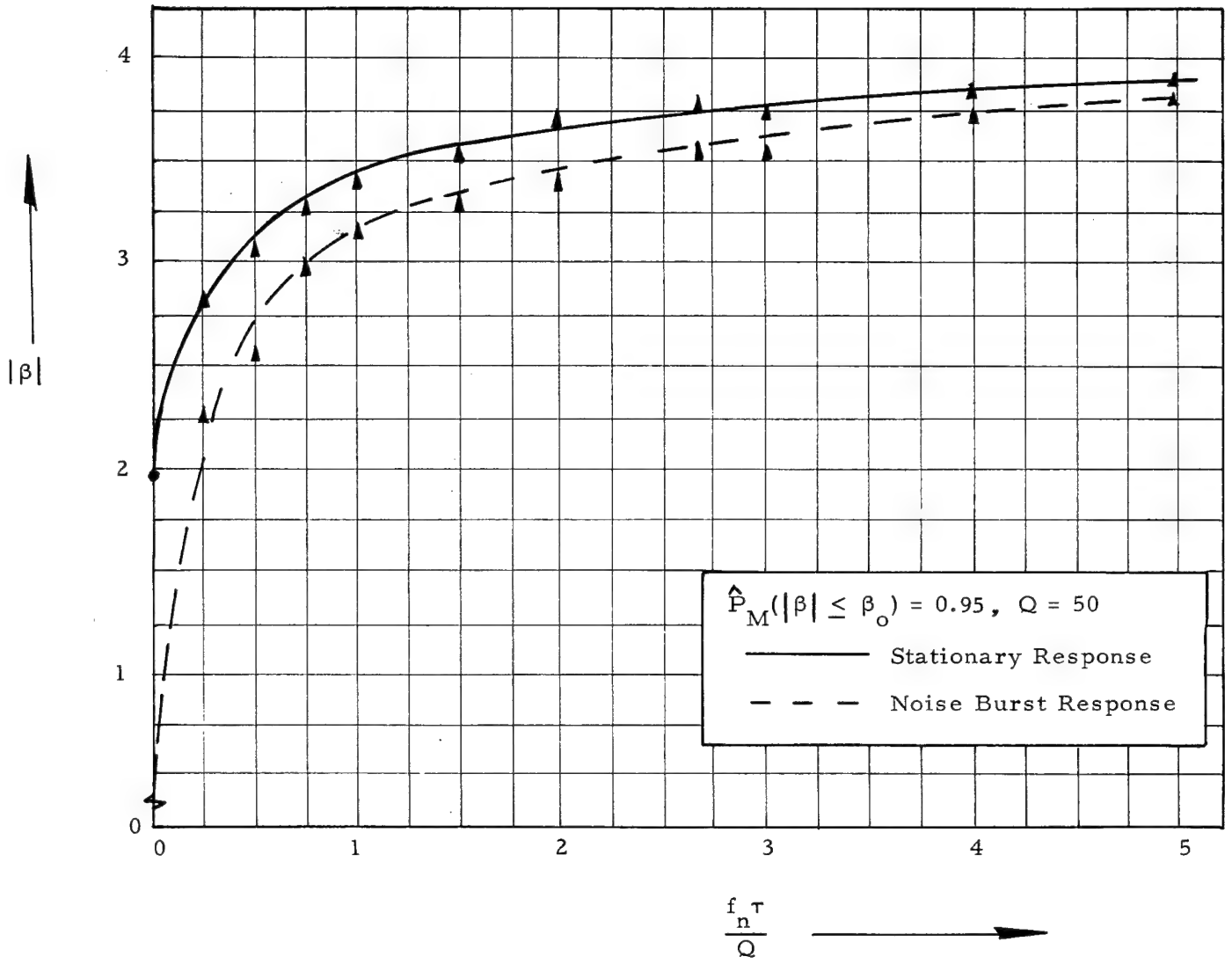

Figure 10. Response Maxima of a Single Degree-of-Freedom System to a Rectangular Burst of White Noise

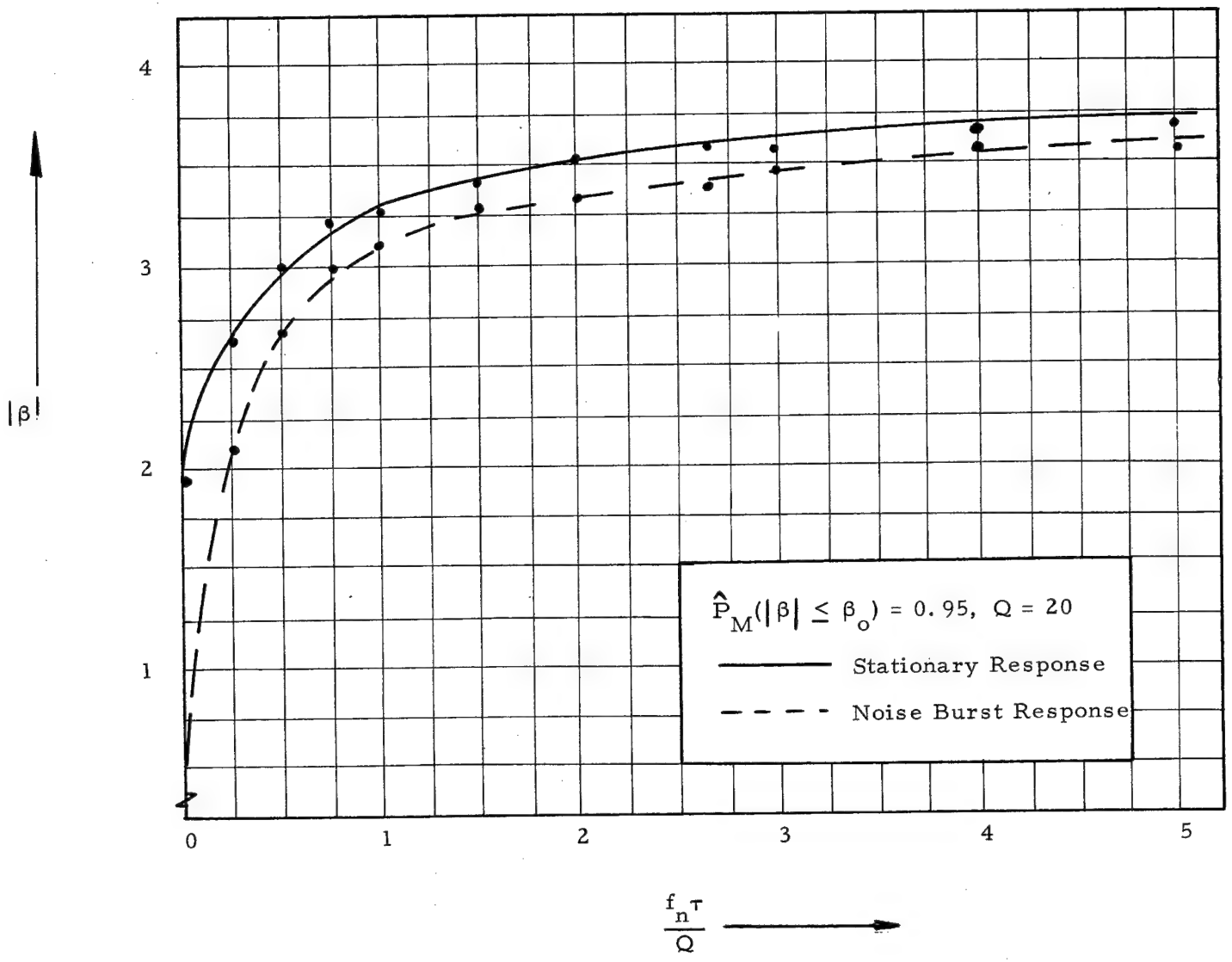

Figure 11. Response Maxima of a Single Degree-of-Freedom System to a Rectangular Burst of White Noise

3. RESPONSE MAXIMA OF DISTRIBUTED ELASTIC PLATES

In this section, the SHP problem is considered wherein the structure is a flat square plate and the applied force excitation is stationary white noise correlated perfectly in both space and time. The β response statistics are then examined via measurements taken at a point near the center of the plate for two types of boundary conditions, (1) simply supported at all edges and (2) rigidly clamped at all edges.

The equation of motion for a flat square plate is

$$D\nabla^4(w) + m\ddot{w} = f(x, y, t) \tag{15}$$

where $f(x, y, t)$ is the applied force excitation per unit area, m the mass per unit area, $w = w(x, y, t)$ = the lateral deflection from static equilibrium, ν the Poisson's ratio and

$$(\ddot{\ }) = \frac{d^2(\ )}{dt^2}$$

$$D = \frac{Eh^3}{12(1 - \nu^2)} \tag{16}$$

$$\nabla^4(\ ) = \left(\frac{\partial^2}{\partial x^2} + \frac{\partial^2}{\partial y^2}\right)^2 (\ )$$

The coefficient D is the flexural rigidity of the plate wherein E is Young's modulus and h the plate thickness. The notation $\nabla^4(\ )$

defines a spatial operator suitable to the rectangular geometry of the square plate where ∇ is the familiar dell operator for rectangular coordinates.

The mean square displacement response of an arbitrary linear elastic structure to a uniform, homogeneous forcing field may be written as

$$\psi_w^2(\vec{r}) = \sum_j \sum_k \phi_j(\vec{r})\, \phi_k(\vec{r}) \int_{-\infty}^{\infty} H_j(\omega)\, H_k^*(\omega)\, L_{jk}(\omega)\, d\omega \tag{17}$$

where the quantity $L_{jk}(\omega)$ is expressed in terms of the spatial cross-spectral density function $S_f(\vec{r}, \vec{r}', \omega)$ as

$$L_{jk}(\omega) = \frac{1}{\overline{M}_j\, \overline{M}_k\, \omega_j^2\, \omega_k^2} \int_0^A \int_0^A \phi_j(\vec{r})\, \phi_k(\vec{r}')\, S_f(\vec{r}, \vec{r}', \omega)\, d\vec{r}\, d\vec{r}' \tag{18}$$

or in terms of the joint acceptance $j_{jk}^2(\omega)$ as

$$L_{jk}(\omega) = \frac{S_f(\vec{r}_o, \omega)\, A^2}{\overline{M}_j\, \overline{M}_k\, \omega_j^2\, \omega_k^2}\, j_{jk}^2(\omega) \tag{19}$$

The notation $\vec{r}$ refers to a spatial position vector, $\phi_j(\vec{r})$ the jth normal mode of the system, ω_j the jth modal frequency, $H_j(\omega)$ the jth modal magnification factor defined as

$$H_j(\omega) = \frac{1}{1 - \left(\frac{\omega}{\omega_j}\right)^2 + i 2\zeta_j \frac{\omega}{\omega_j}} \tag{20}$$

and $H_k^*(\omega)$ the complex conjugate of $H_k(\omega)$. The symbol A denotes the area of the plate and the quantity $S_f(\vec{r}_o, \omega)$ refers to a spectral density function of the applied force at the spatial location $\vec{r}_o$. If the position $\vec{r}_o$ is selected to be a point on the structure where $S_f(\vec{r}_o, \omega)$ is a maximum, $j_{jk}^2(\omega)$ will vary from zero to one. From Eqs. (18) and (19), the joint acceptance is found to be

$$j_{jk}^2(\omega) = \frac{1}{S_f(\vec{r}_o, \omega)\, A^2} \int_0^A \int_0^A \phi_j(\vec{r})\, \phi_k(\vec{r}')\, S_f(\vec{r}, \vec{r}', \omega)\, d\vec{r}\, d\vec{r}' \tag{21}$$

By assuming the $j \neq k$ terms to be negligible in comparison to the $j = k$ terms, the mean square displacement response becomes (for the conditions of this problem)

$$\psi_w^2(\vec{r}) \simeq S_o \sum_j \frac{\phi_j^2(\vec{r}) \left[\int_0^A \phi_j(\vec{r})\, d\vec{r}\right]^2}{\overline{M}_j^2\, \omega_j^4} \int_{-\infty}^{\infty} \left|H_j(\omega)\right|^2 d\omega \tag{22}$$

or, in terms of the physically realizable spectrum G_o,

$$\psi_w^2(\vec{r}) = G_o \sum_j \frac{\phi_j^2(\vec{r}) \left[\int_0^A \phi_j(\vec{r})\, d\vec{r} \right]^2}{\overline{M}_j^2\, \omega_j^4} \int_0^\infty \left| H_j(\omega) \right|^2 d\omega \qquad (23)$$

Similarly, the mean square velocity response may be written as

$$\psi_{\dot{w}}^2(\vec{r}) = G_o \sum_j \frac{\phi_j^2(\vec{r}) \left[\int_0^A \phi_j(\vec{r})\, d\vec{r} \right]^2}{\overline{M}_j^2\, \omega_j^2} \int_0^\infty \left(\frac{\omega}{\omega_j} \right)^2 \left| H_j(\omega) \right|^2 d\omega \qquad (24)$$

In terms of the functions I_n and II_n shown as Figure 3 and 4, Eqs. (23) and (24) are of the form

$$\psi_w^2(\vec{r}) = \frac{\pi}{2} G_o \sum_j \phi_j^2(\vec{r}) \left[\int_0^A \phi_j(\vec{r})\, d\vec{r} \right]^2 \frac{Q_j (I_n)_j}{\overline{M}_j^2\, \omega_j^3} \qquad (25)$$

$$\psi_{\dot{w}}^2(\vec{r}) = \frac{\pi}{2} G_o \sum_j \phi_j^2(\vec{r}) \left[\int_0^A \phi_j(\vec{r})\, d\vec{r} \right]^2 \frac{Q_j (II_n)_j}{\overline{M}_j^2\, \omega_j} \qquad (26)$$

The SHP problem for the plate structure is studied empirically by examining the β results from the electrical analog simulation depicted schematically by Figure 12. The transformer whiffle-tree circuit is used to create a spatial correlation of unity for the white noise excitation which is applied to the plate analog. As shown in this figure, the data of interest include both positive and negative response maxima (measured by the "peak" readers) and the RMS response.

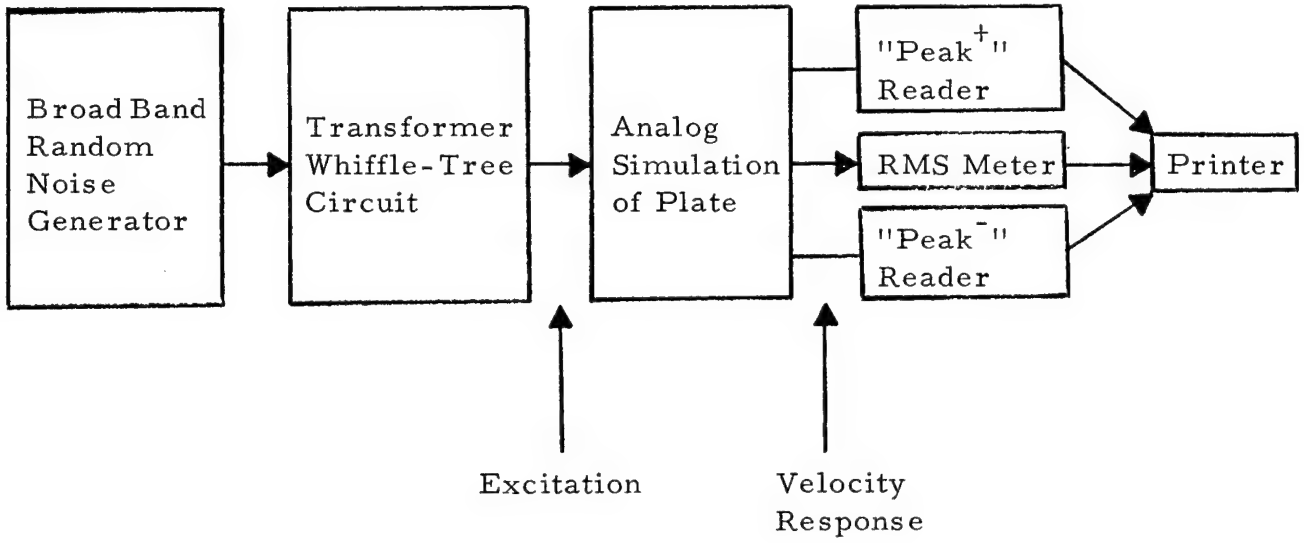

Figure 12. Block Diagram of Analog Simulation Study

The plate analog circuits are derived from energy concepts (Reference 2) and may be categorized as mobility analogs. Such circuits consist of passive electrical components, are appropriate for nonuniform physical and geometric properties, and appear topologically similar* to the physical system. Mathematically, this type of analog corresponds to a finite-difference model whereas, mechanically, it may be interpreted as a form of lumped-parameter model. Background information about such structural analogs is found in Reference 9.

The physical dimensions and physical properties of the uniform, homogeneous plate are defined as

*For the more complicated structural configurations, a rather vivid imagination admittedly is required.

$$a = b = \ell = 11 \text{ in}$$

$$h = 0.0625 \text{ in}$$

$$E = 10.5 \times 10^6 \text{ lb/in}^2$$

$$\rho = 0.10 \text{ lb/in}^3$$

$$\nu = 0.3$$

For simply supported edge conditions, the plate modal frequencies are given by

$$f_{rs} = \frac{\pi}{2} \sqrt{\frac{D}{m}} \left[\left(\frac{r}{a} \right)^2 + \left(\frac{s}{b} \right)^2 \right] \text{ cps} \qquad (27)$$

where rs denote the mode numbers (the number of half-sines in the x and y dimensions). With D = 235 lb-in and $m = 1.62 \times 10^{-5}$ lb-sec^2/in^3, the fundamental modal frequency is $f_{11} \simeq 99$ cps. For rigidly clamped edge conditions, the fundamental modal frequency is $f_{11} \simeq 181$ cps.

The plate circuits and expressions for the component values used in this study are given in Reference 3. By scaling the analog circuits such that electrical time corresponds to real time (N = 1) and applying a uniformly distributed sinusoidal load, the velocity to force frequency response functions at $x = \frac{4\ell}{9}$ and $y = \frac{4\ell}{9}$ are obtained as shown in Figure 13. These response functions indicate the magnitude of the circuit impedance at a particular point and are equivalent to mobility plots (magnitude only). The fundamental modal frequencies are noted to be approximately equal to the values previously calculated for both simply supported and rigidly clamped boundary conditions. Due to the symmetry of the loading, only even valued modes (i. e. where the mode shapes are symmetric about the

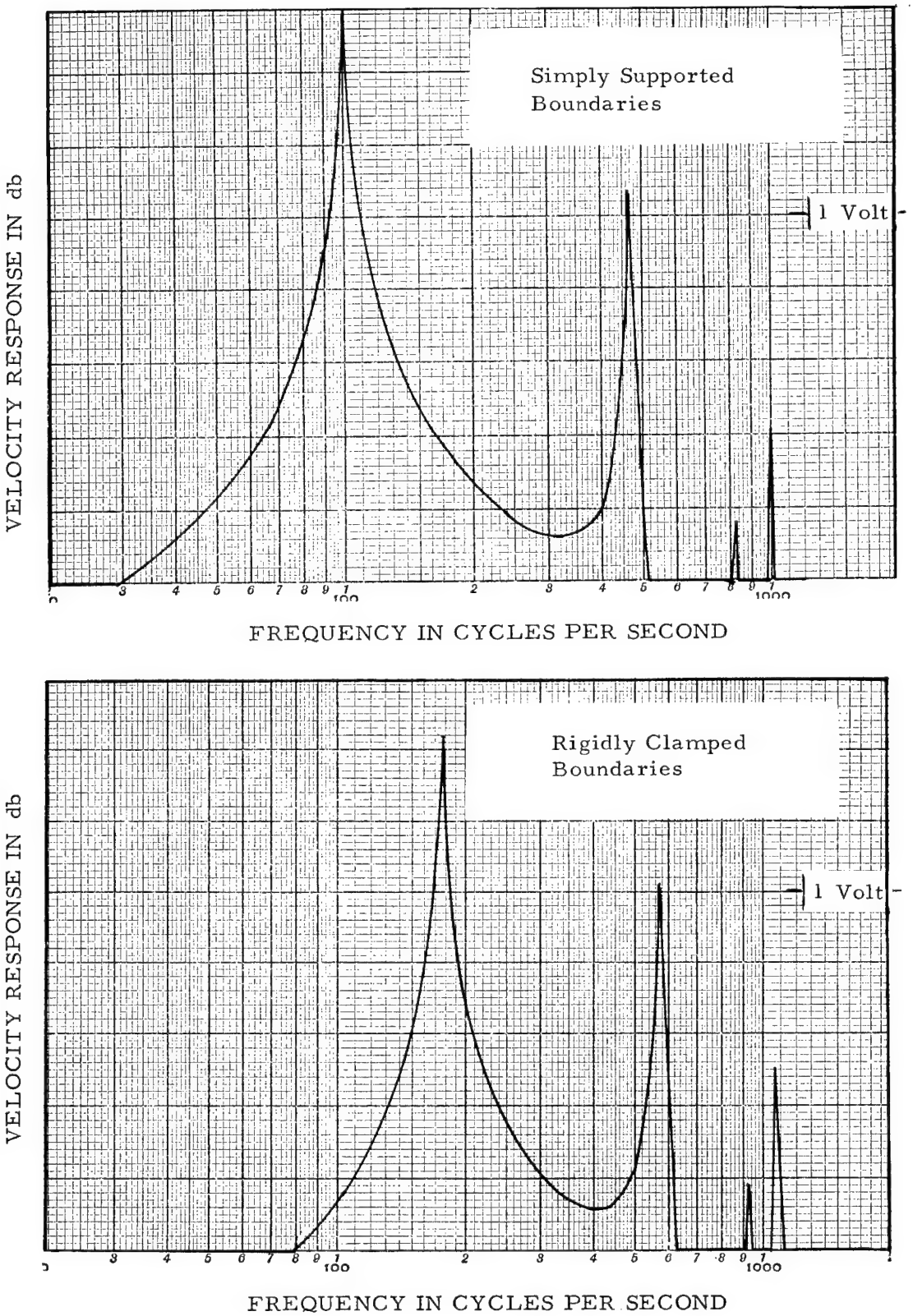

Figure 13. Frequency Response Functions of a Square Plate

mid-spans of the plate) can be excited as is seen in these plots. The depth of the valleys between the modal frequencies is indicative of the modal coupling in the system.

A measure of the damping in the first mode is given by

$$Q_{11} = \frac{f_{11}}{\Delta f_{11}} \tag{28}$$

where Δf_{11} is the half-power bandwidth centered at f_{11}. This expression yields $Q_{11} \simeq 33.9$ for the simply supported boundaries and $Q_{11} \simeq 39.7$ for the rigidly clamped boundaries. Such damping is inherent in the computer (due to the fact that the circuit capacitors, inductors and transformers are not ideal, interconnecting wires have resistance, physical layout of the components produce parasitics, etc.) and, although it cannot be precisely controlled, damping values in the first mode ranging from $Q = 30$ to $Q = 50$ are to be expected with proper scaling.

In the simulation study, the plate is continuously excited by stationary white noise correlated perfectly in both space and time and the velocity response at $x = \frac{4\ell}{9}$ and $y = \frac{4\ell}{9}$ is observed for various time durations T such that the dimensionless ratio $f_{11}T/Q_{11}$ ranges from 0 to 5.00. The magnitude of the white noise input is adjusted such that a response maxima of approximately six times the RMS response ($6\beta_o$ values) could occur without distortion. For a specified T value, the response is sampled 100 times wherein both the positive and negative response maxima are recorded for each sampling thus producing a total of 200 data points. Typical response time histories (as observed over a finite sampling time interval T) are shown as Figures 14 and 15. It is to be noted the response does not appear to be the same as the stationary response of a linear oscillator to white noise, i.e., as a type of harmonic motion with randomly varying amplitude and phase. Rather, higher frequency effects due to modal frequencies other than f_{11} are evident.

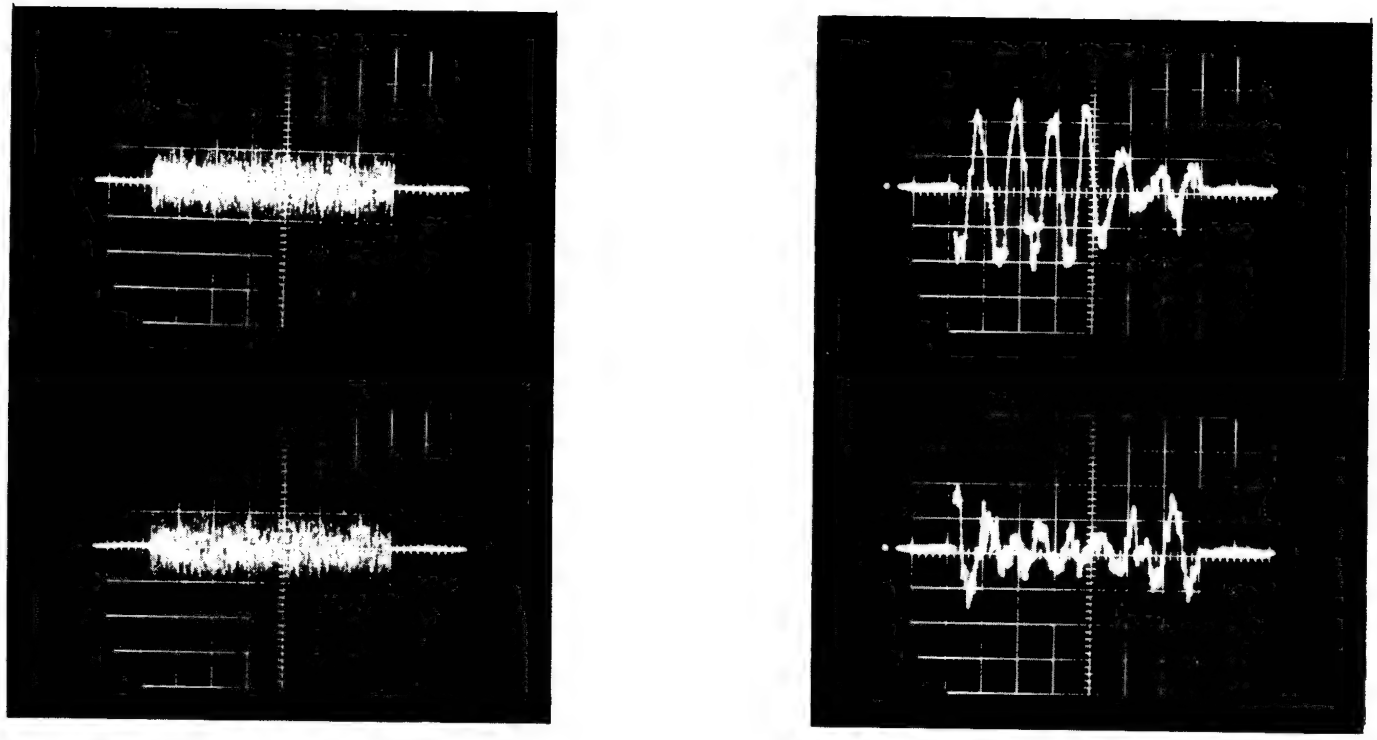

Stationary White Noise Excitation

Velocity Response

Figure 14. Response of a Square Plate to Stationary White Noise with a Spatial Correlation of Unity — Simply Supported Boundaries

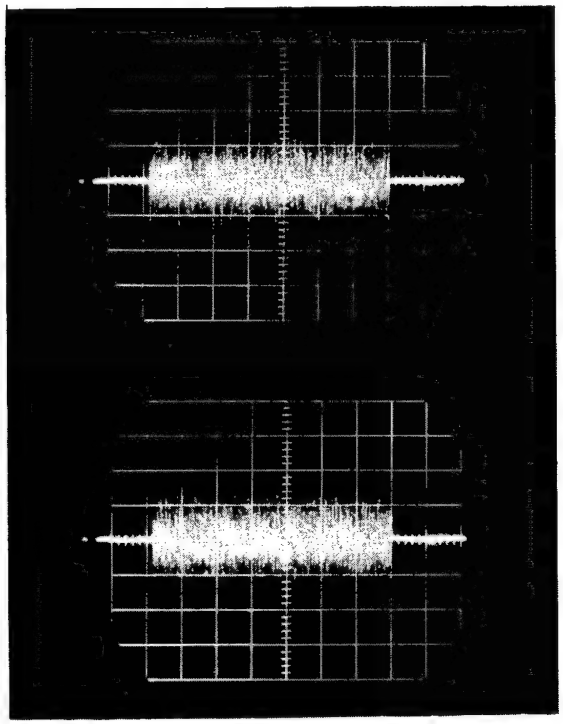

Stationary White Noise Excitation

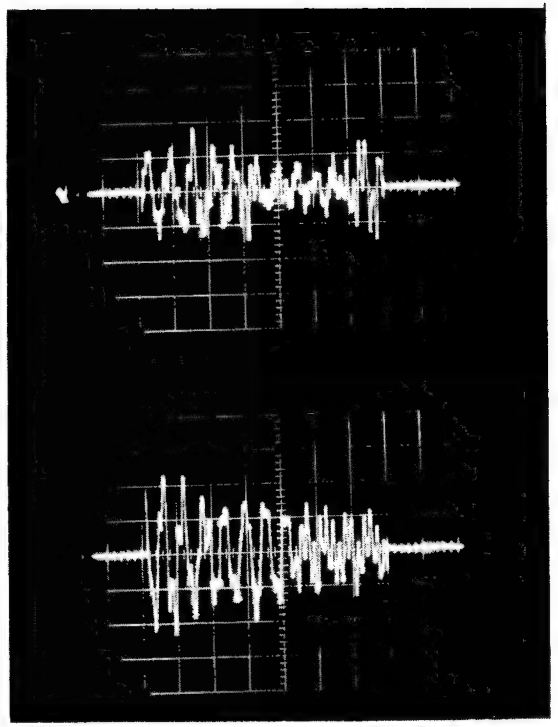

Velocity Response

Figure 15. Response of a Square Plate to Stationary White Noise with a Spatial Correlation of Unity — Rigidly Clamped Boundaries

These individual maxima response data are next arranged in rank order, then divided by the RMS response to form histograms of $\hat{P}_M(\beta^+ \leq \beta_o)$ and $\hat{P}_M(\beta^- \leq \beta_o)$. A typical example of such data is shown as Figure 16. By adding the β^+ and β^- data, a histogram of $\hat{P}_M(|\beta| \leq \beta_o)$ is formed as shown in Figure 17 and this is used (one such histogram for each sampling time T) to obtain individual probability data points for $|\beta|_o$ versus $f_{11}T/Q_{11}$ plots. It is understood that these histograms are estimates of the true maxima response probability density functions for a specified value of $f_{11}T/Q_{11}$. Additional data should therefore be accumulated so that the variance of such data may be analyzed.

Following such an empirical procedure just described, the $|\beta|$ versus $f_{11}T/Q_{11}$ plots of Figures 18 and 19 are developed. Note that only the fundamental modal frequency f_{11} and its associated damping Q_{11} need be known for the structure. These curves display a behavior similar to that for the single degree-of-freedom system (compare with Figures 8 and 9) but have consistently higher values of $|\beta|$ for a given probability. The curve for $\hat{P}_M(|\beta| \leq \beta_o) = 0.50$ is approximately the same as that for the average $|\beta|$ and consequently is not included as a separate figure.

For a given probability, the $|\beta|_o$ ratio increases indefinitely with time and theoretically $|\beta| \rightarrow \infty$ as $T \rightarrow \infty$, the latter being a truism of limited practical concern. The greatest rate of increase in $|\beta|$ is seen to occur within $0 \leq f_{11}T/Q_{11} \leq 3$. For $f_{11}T/Q_{11} \simeq 3$, $|\beta|$ values of approximately three are expected on the average and 95% of all amplitude maxima are expected to be equal to or less than $\beta_o \simeq 4$.

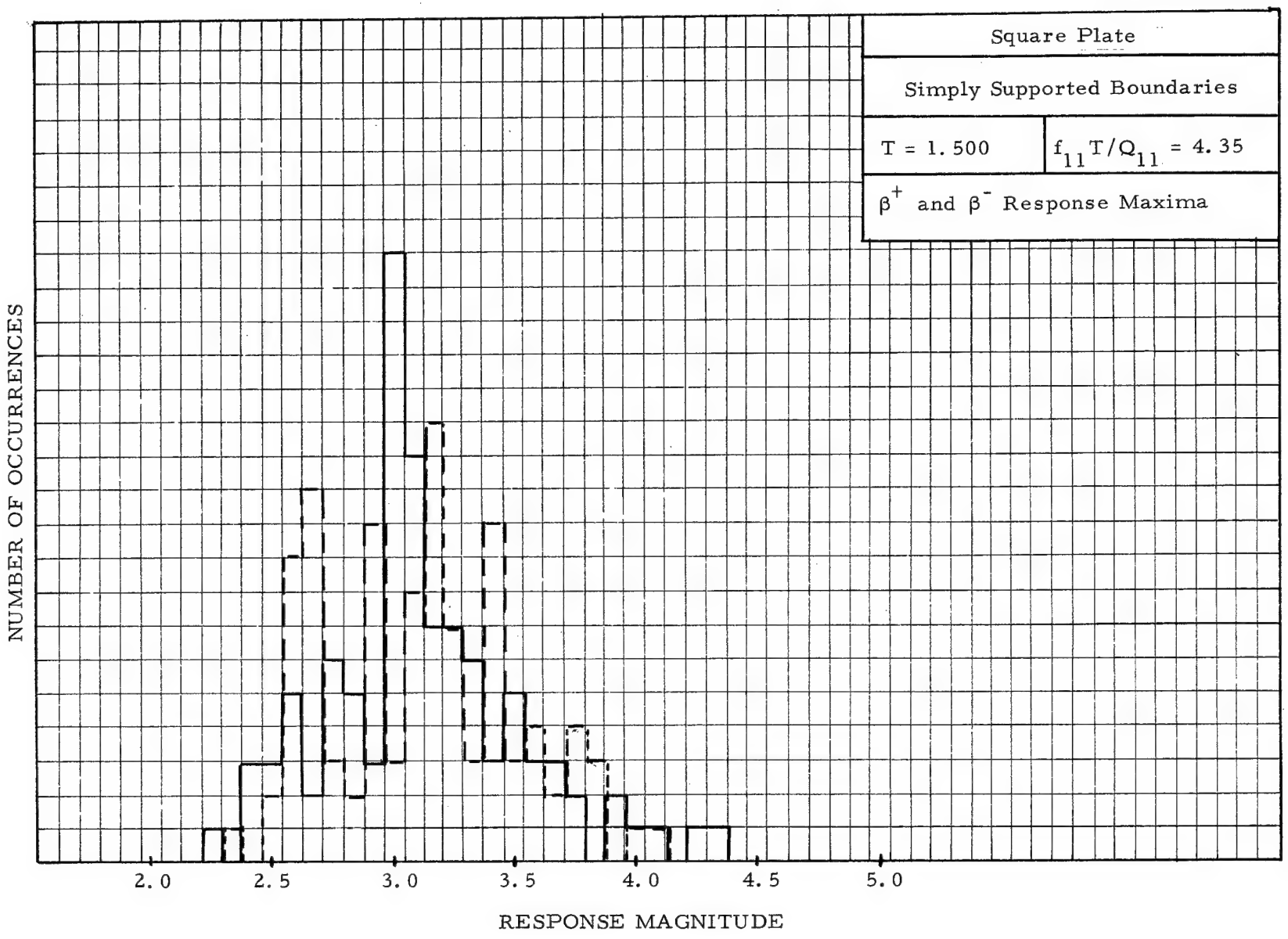

Figure 16. Histogram of Maximum Response Data

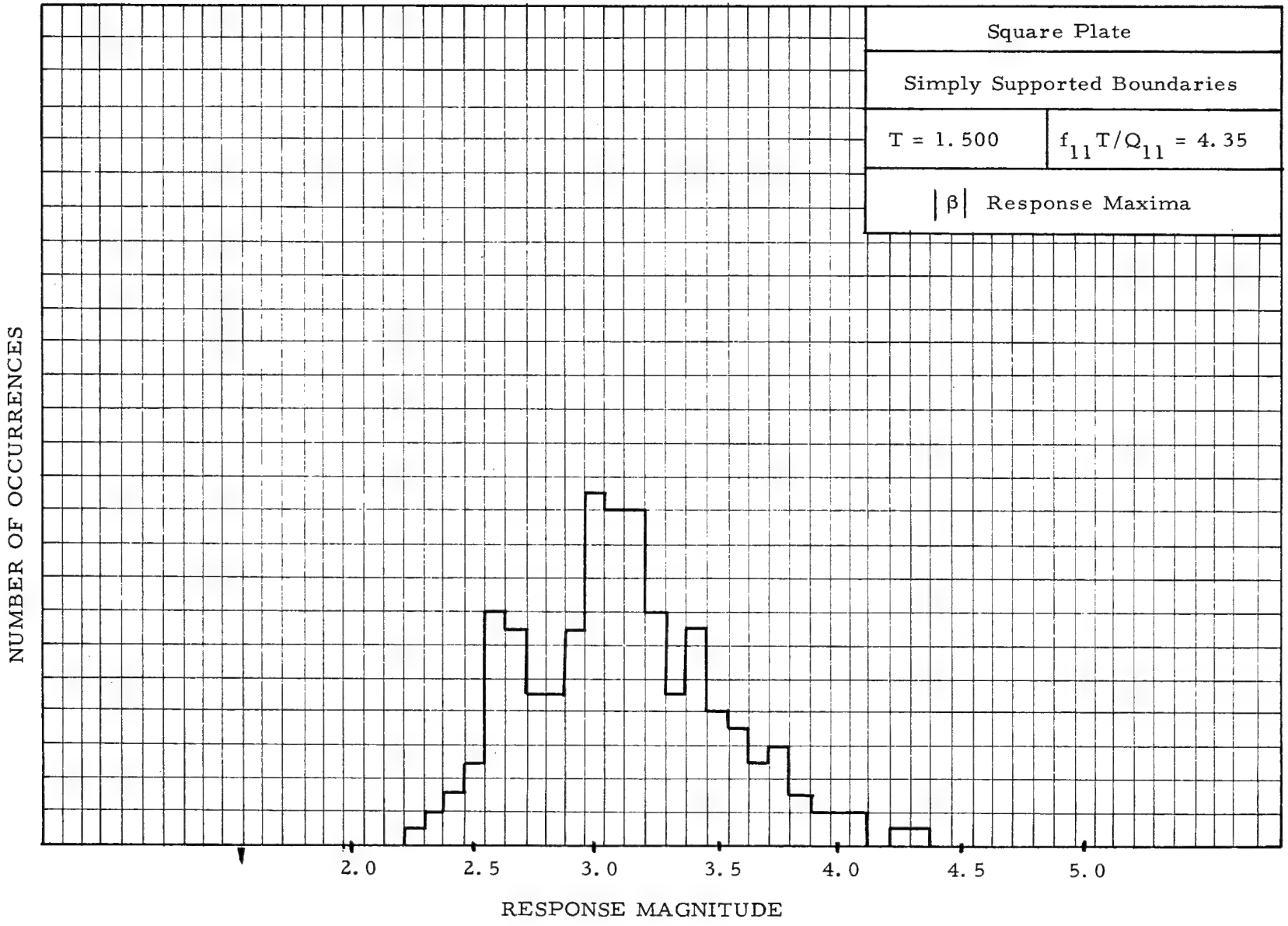

Figure 17. Histogram of Maximum Response Data

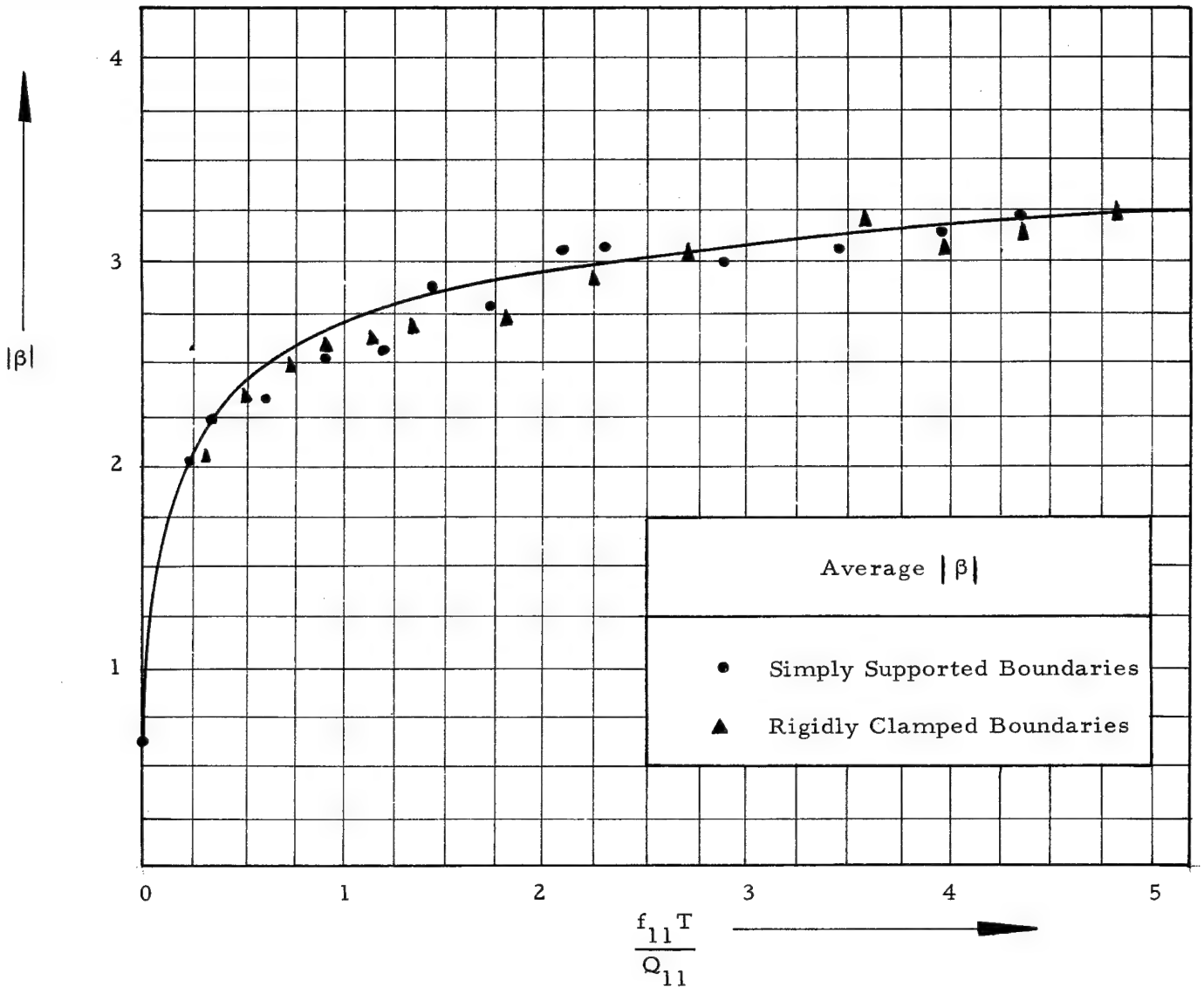

Figure 18. Maximum Response of a Square Plate to White Noise Correlated Perfectly in Space and Time

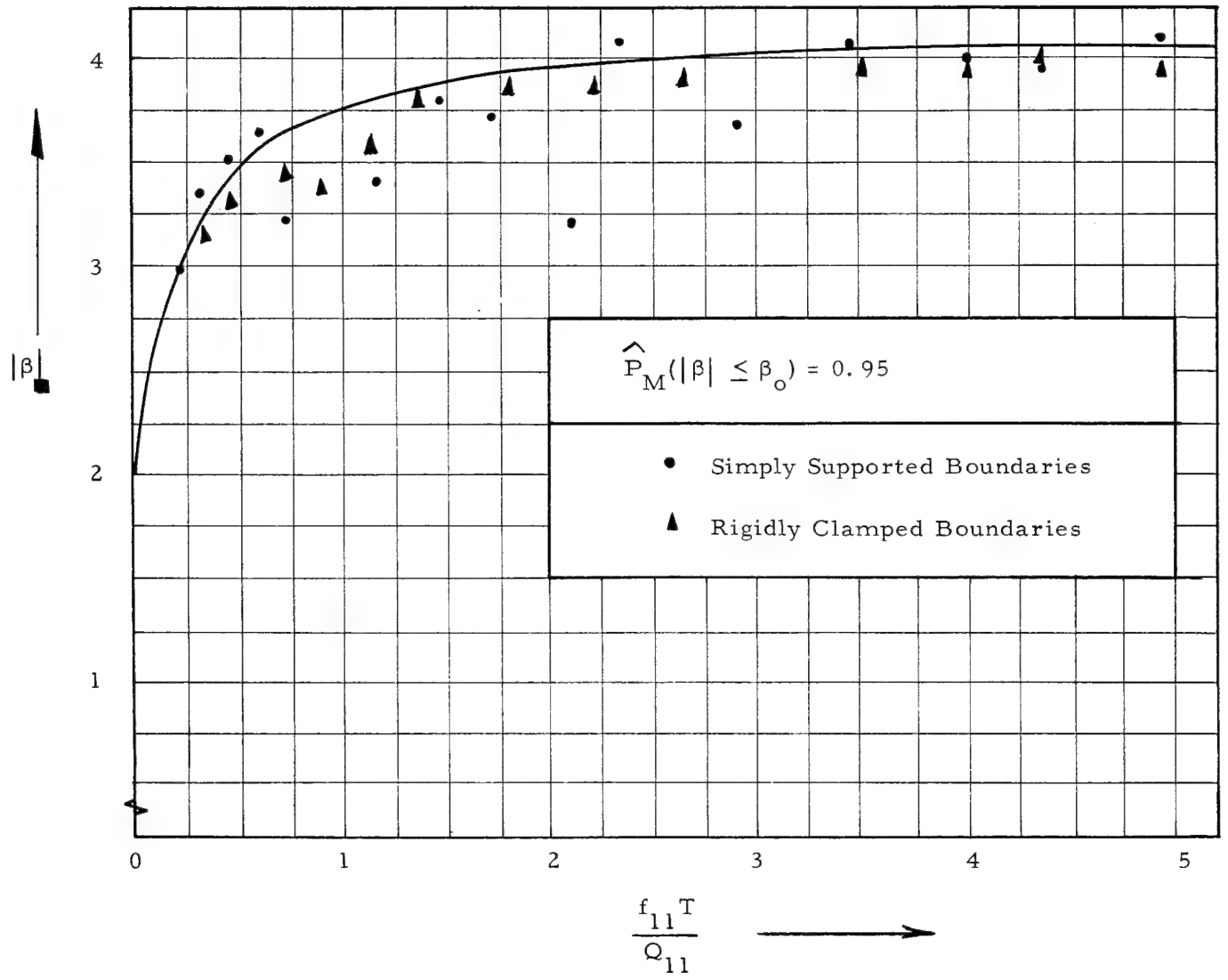

Figure 19. Maximum Response of a Square Plate to White Noise Excitation Correlated Perfectly in Space and Time

Consider the maximum response characteristics of a plate subjected to a burst of white noise shaped in time by a well defined envelope function. It is required to develop a solution such that one may predict the expected single highest response maximum due to a noise burst of finite duration. This problem may be examined in much the same way as with the stationary excitation, that is by an analog simulation study wherein data for the response maxima are collected and arranged to form $|\beta|$ plots. However, special attention must be given to (1) the RMS response used to form the β ratio and (2) the time duration common to the dimensionless time parameter $f_{11}T/Q_{11}$. As with the previous problem, the β response is normalized using the RMS response of the system to broadband white noise correlated perfectly in both space and time wherein the magnitude of the stationary noise corresponds to the value where the envelope function is a maximum ($E(t) = 1$). Although admittedly arbitrary, this procedure avoids consideration of a time varying RMS. The sampling time interval T is replaced by τ which denotes the time duration of the noise burst. With these modifications in definition, this nonstationary problem may now be plausibly attacked.

With the system initially at rest, a rectangular noise burst is applied for τ seconds typically producing the response as shown in Figure 20. The system response is monitored from the onset of the excitation until the free vibration response has decayed to a negligible level and both the positive and negative maximum response values are recorded. By sampling the system response one hundred times for each τ setting and arranging the data in the same manner as with the stationary excitation, the $|\beta|$ plots of Figures 21 and 22 are constructed. Data points for simply supported boundaries are noted by •'s and data points for rigidly clamped boundaries are shown by ▲'s.

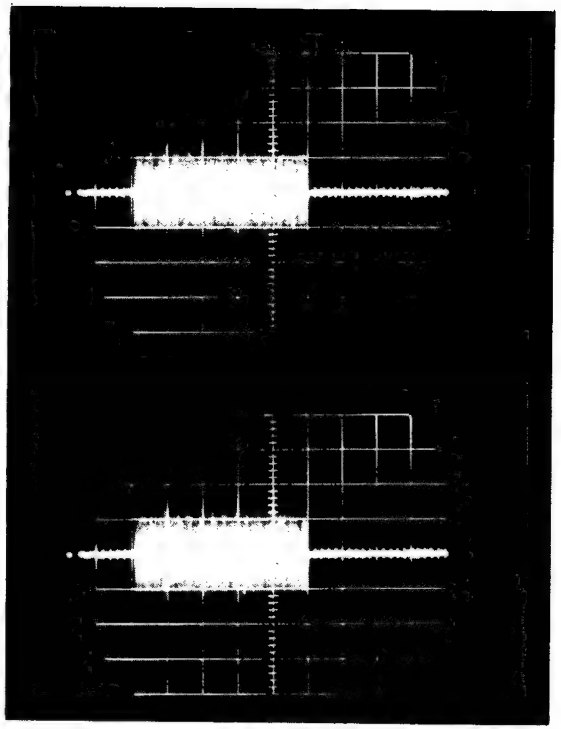

Noise Burst Excitation

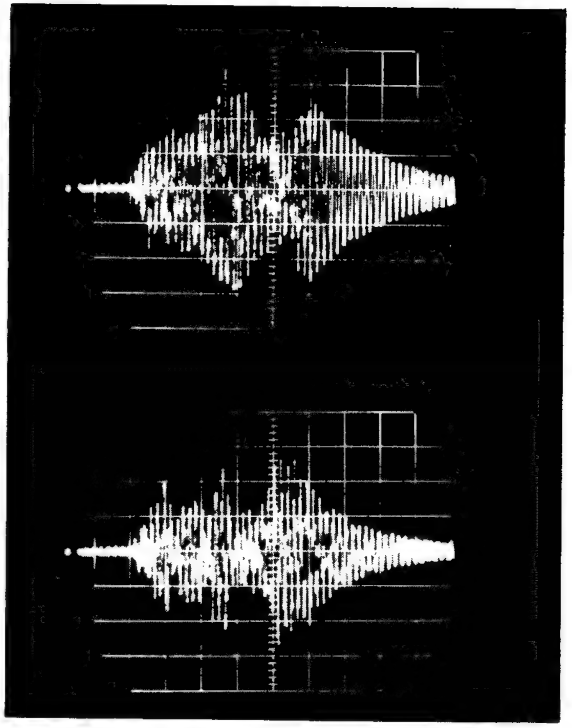

Velocity Response

Figure 20. Typical Response of a Square Plate to Rectangular Bursts of White Noise Correlated Perfectly in Space and Time

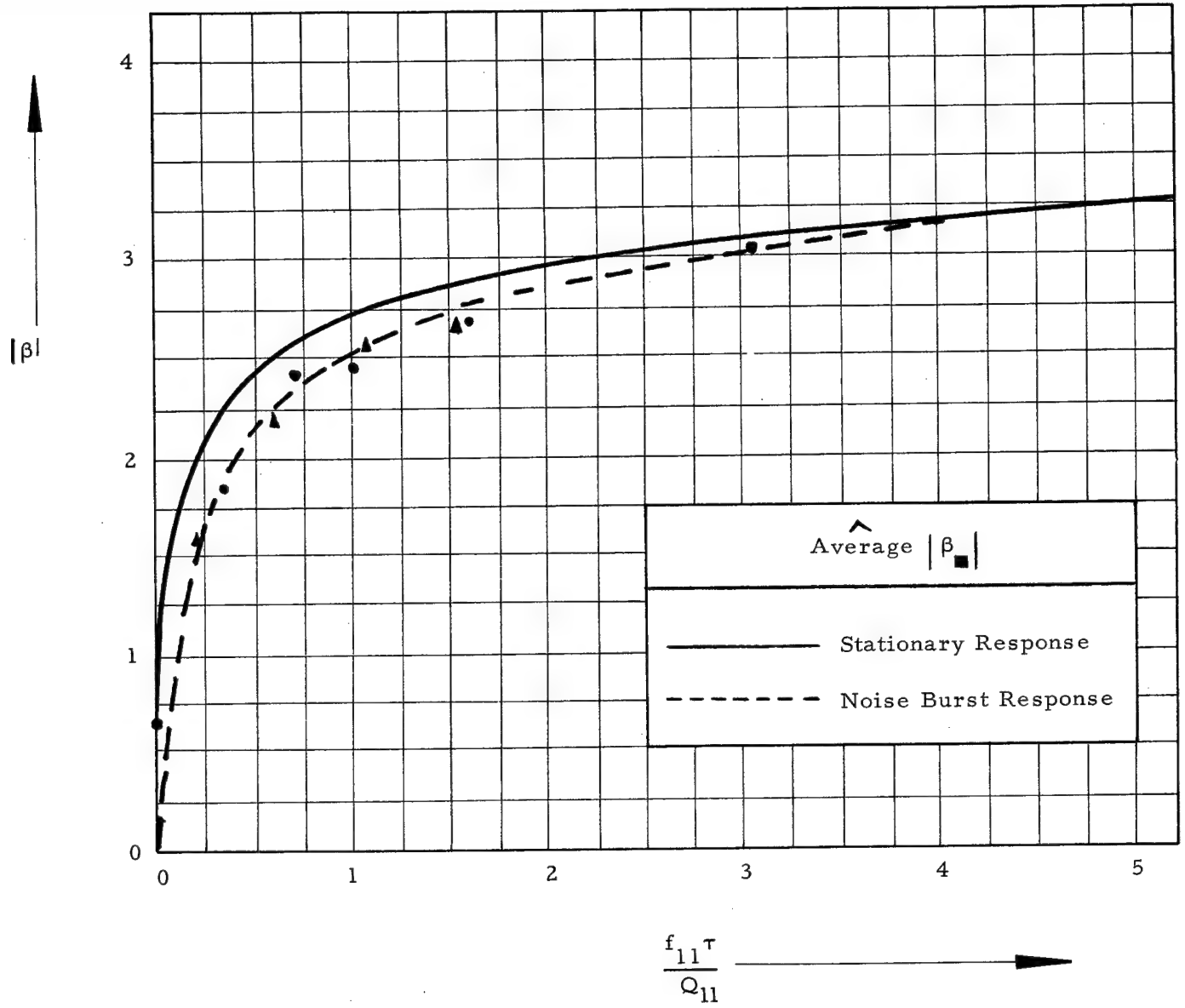

Figure 21. Maximum Response of a Square Plate to Rectangular Bursts of White Noise Correlated Perfectly in Space and Time

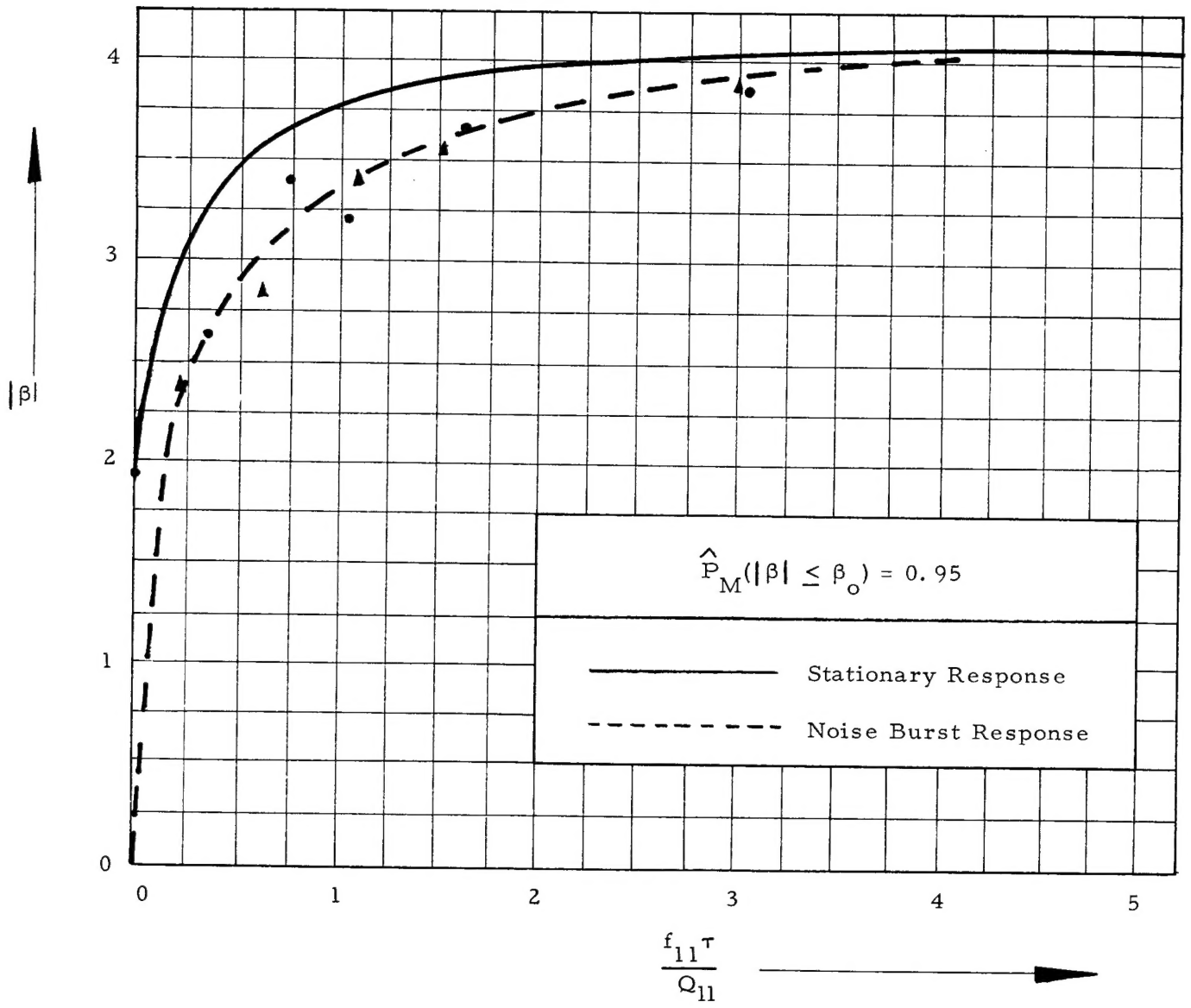

Figure 22. Maximum Response of a Square Plate to Rectangular Bursts of White Noise Correlated Perfectly in Space and Time

Similar to the behavior for a single degree-of-freedom system, the response data are bounded by the curve depicting the stationary response of the plates. As the time duration of the noise burst becomes long relative to the fundamental modal period of the structure, the nonstationary excitation appears as a stationary white noise input and the noise burst response becomes essentially that of the stationary curve. Curves such as these may be used to define the conditions under which a multimode system excited by a noise burst achieves stationarity in its response.

Of vast importance, however, is that the data for both stationary and nonstationary random excitation imply the $|\beta|$ response tends to be independent of the boundary conditions. Such a statement must be considered as a qualified conjecture until more data are collected and analyzed and/or theoretical work is advanced to support or reject this claim. In the interim, $|\beta|$ curves such as included in this report may be used discretely in engineering applications wherein a maxima response criteria for distributed structures is applicable.

4. CONCLUDING REMARKS

The SHP problem has been reviewed briefly for a single degree-of-freedom system wherein both analytical and empirical solutions have been discussed. More important, data have been presented forming an empirical solution to the SHP problem for a square plate with (1) simply supported boundaries and (2) rigidly clamped boundaries. The random excitation applied over the plate is (1) stationary white noise with a unity correlation in both space and time.and (2) nonstationary excitation shaped (in time) as rectangular noise bursts with a unity correlation in both space and time. A comparison of $\hat{P}_M(|\beta| \leq \beta_o)$ data for the single degree-of-freedom system and plate shows the $|\beta|$ response maxima to be consistently higher for the plate. Of particular significance in the plate data is the implication that the $\hat{P}_M(|\beta| \leq \beta_o)$ curves are independent of the boundary conditions. Such an implication has far-reaching practical significance and should be investigated thoroughly in the immediate future. In addition, the effect on the response maxima of mass loading and of bandlimited excitation with spatial and spectral characteristics more typical of service conditions would be indeed worthwhile investigations.

ACKNOWLEDGMENTS

The diligent assistance of Messrs. J. M. McMullin and J. M. Trull in conducting the analog simulation is acknowledged with thanks. Both are affiliated currently with the CEAC Computer Section of the McDonnell Aircraft Company.

REFERENCES

1. Aspinwall, D. M., "An Approximate Distribution for the Maximum Response During Random Vibration," AIAA Simulation for Aerospace Flight Conference, New York, 1963, pp 326-330.

2. Barnoski, R. L., "Basic Analog Circuits for Two-Dimensional Distributed Elastic Structures," NASA CR-667, National Aeronautics and Space Administration, Washington, D. C., January 1967.

3. Barnoski, R. L., "Dynamic Characteristics of Distributed Structures by Passive Analog Simulation," AIAA Paper No. 67-40, AIAA 5th Aerospace Sciences Meeting, New York, 1967.

4. Barnoski, R. L., "The Maximum Response of a Linear Mechanical Oscillator to Stationary and Nonstationary Random Excitation," NASA CR-340, National Aeronautics and Space Administration, Washington, D. C., December 1965.

5. Crandall, S. H., K. L. Chadiramani and R. G. Cook, "Some First-Passage Problems in Random Vibration," Transactions of the ASME Journal of Applied Mechanics, Paper No. 66-APM-Y.

6. Crandall, S. H. and W. D. Mark, Random Vibration in Mechanical Systems, New York, Academic Press, 1963.

7. Gray, C. L., "First Occurrence Probabilities for Extreme Random Vibration Amplitudes," The Shock and Vibration Bulletin, No. 35, Part 4, February 1966, pp 99-104.

8. MacNeal, R. H., R. L. Barnoski and J. A. Bailie, "Response of a Simple Oscillator to Nonstationary Random Noise," Journal of Spacecraft and Rockets, Vol. 3, No. 3, March 1966, pp. 441-443.

9. MacNeal, R. H., Electric Circuit Analogies for Elastic Structures, New York, J. Wiley & Sons, Inc., 1962.

10. Mark, W. D., "On False-Alarm Probabilities of Filtered Noise," Proceedings of the IEEE, Vol. 54, No. 2, February 1966, pp 316-317.

11. Roberts, J. B., "The Response of a Simple Oscillator to Band-Limited White Noise," Report No. 65/3, University College, London, Department of Mechanical Engineering, London, W. C. T., May 1965.